

## A Flexible Approach for the Calibration of Biplanar Radiography of the Spine on Conventional Radiological Systems

Daniel C. Moura<sup>1</sup>, Jorge G. Barbosa<sup>1</sup>, Ana M. Reis<sup>2</sup>  
João Manuel R. S. Tavares<sup>3</sup>

**Abstract:** This paper presents a new method for the calibration of biplanar radiography that makes possible performing 3D reconstructions of the spine using conventional radiological systems. A novel approach is proposed in which a measuring device is used for determining focal distance and have a rough estimation of translation parameters. Using these data, 3D reconstructions of the spine with correct scale were successfully obtained without the need of calibration objects, something that was not previously achieved. For superior results, two optional steps may be executed that involve an optimisation of the geometrical parameters, followed by a scale adjustment with a very simple calibration object.

Computer simulations with *in vivo* CT data show RMS 3D reconstruction errors of 1.9 mm when under the maximum expected variation of the geometrical parameters of the radiological system. Simulations also show that the 3D spinal length may be accurately calculated, but with superior results when using optimisation and adjusting scale (RMS error of 2.09 mm). *In vitro* experiments with a dried spine composed by 17 vertebrae show mean 3D reconstructions errors of 1.7 mm.

We conclude that the proposed method is suitable for use in clinical environment, and that it compares favourably with previous calibration techniques.

**Keywords:** Medical imaging, X-ray imaging, Calibration, Geometric Modeling, Optimisation.

---

<sup>1</sup> Universidade do Porto, Faculdade de Engenharia, Departamento de Engenharia Informática, and Laboratório de Inteligência Artificial e de Ciência de Computadores, Porto, Portugal, Email: {daniel.moura, jbarbosa}@fe.up.pt

<sup>2</sup> Serviço Médico de Imagem Computorizada, Porto, Portugal

<sup>3</sup> Universidade do Porto, Faculdade de Engenharia, Departamento de Engenharia Mecânica, and Instituto de Engenharia Mecânica e Gestão Industrial, Porto, Portugal, Email: tavares@fe.up.pt

## 1 Introduction

Three-dimensional (3D) reconstructions of the spine are necessary for a proper evaluation of spinal deformities, such as idiopathic scoliosis. These deformities have a 3D nature that cannot be conveniently assessed by planar radiography. Examples of clinical indexes that can only be quantified with a 3D model of the spine include the maximum plane of curvature, vertebrae axial rotation [Stokes (1994)], and the three-dimensional spinal length [Papin, Labelle, Delorme, Aubin, De Guise, and Dansereau (1999)]. Additionally, 3D reconstructions of the spine are important for making personalised biomechanical models of patients' spines that may be used for guiding therapy (e.g. [Perie, Aubin, Petit, Beausejour, Dansereau, and Labelle (2003); Périé, Aubin, Lacroix, Lafon, and Labelle (2004); Labelle, Bellefleur, Joncas, Aubin, and Cheriet (2007)]). With other anatomic structures, conventional 3D imaging techniques, such as Computer Tomography (CT) and Magnetic Resonance Imaging (MRI), may be used for these purposes (e.g. [Yang, Tang, Yuan, Hatsukami, Zheng, and Woodard (2007); Yang, Tang, Yuan, Kerwin, Liu, Canton, Hatsukami, and Atluri (2008)]). However, these 3D imaging techniques are not suitable for capturing the global shape of the spine because they require patients to be lying down, which alters the spine configuration. Additionally, they are more expensive and, in the case of CT, the doses of ionising radiation required for a full scan are inappropriate for patients. For all these reasons, 3D reconstructions of the spine are usually done using multiple radiographs from different planes.

Several methods have been proposed for accomplishing 3D reconstructions of the spine from radiographs. The most well-known techniques require a set of point-matches to be manually identified by an expert in two radiographs (i.e. frontal and lateral planes). In [Aubin, Describes, Dansereau, Skalli, Lavaste, and Labelle (1995)] a set of 6 stereo-corresponding points per vertebra are used (i.e. centre of superior and inferior endplates, and the superior and inferior extremities of the pedicles), and in [Mitton, Landry, Veron, Skalli, Lavaste, and De Guise (2000)] this set is augmented with non-stereo corresponding points for better capturing vertebrae shape. Finally, in [Pomero, Mitton, Laporte, de Guise, and Skalli (2004)], the number of landmarks was decreased to 4 per vertebrae per radiograph due to the use of statistical models. More recently, other techniques are urging for reducing user-interaction even further that are based on the identification of the spine midline through the use of splines [Dumas, Blanchard, Carlier, de Loubresse, Le Huec, Marty, Moinard, and Vital (2008); Humbert, Guise, Aubert, Godbout, and Skalli (2009); Kadoury, Cheriet, and Labelle (2009); Moura, Boisvert, Barbosa, and Tavares (2009)]. There are also attempts of quasi-unsupervised methods, but only for the lower part of the spine [Benameur, Mignotte, Labelle, and Guise

(2005); Benameur, Mignotte, Parent, Labelle, Skalli, and de Guise (2003)].

Independently of their specific approach, all these methods need to know the geometry of the radiological system, including the patient position and orientation, in order to compute 3D data from the 2D data of the planar radiographs. This is achieved using calibration methods. In most of the clinical institutions where bi-planar radiography is utilised for performing 3D reconstructions of the spine, the calibration methods that are used require very specific equipment and dedicated x-ray machinery, which makes them expensive. This is the case of the method described in [Dansereau and Stokes (1988)] that uses a calibration cage that surrounds the patient and a rotatory platform for positioning the patient. In this work, calibration was accomplished using the Direct Linear Transform (DLT) technique [Abdel-Aziz and Karara (1971)], which has significant extrapolation errors [Wood and Marshall (1986)]. Therefore, the calibration object was built large enough to contain, within its limits, the anatomical structures that are being reconstructed. In [Dumas, Mitton, Laporte, Dubousset, Steib, Lavaste, and Skalli (2003)], a very large calibration apparatus was also used with a rotatory platform that tries to be more patient-friendly, while achieving comparable accuracy. Finally, in [Cheriet, Laporte, Kadoury, Labelle, and Dansereau (2007)] it was proposed the use of a calibration jacket with 16 radiopaque markers, but which also needs a rotatory platform that includes a calibration object with another 6 radiopaque pellets. While this last method is able of handling patient motion between acquisitions, which was one of the problems of the previous techniques, it still needs a fixed radiological setup with dedicated equipment. This makes these methods unsuitable for massive clinical use. Additionally, the content of radiographs is perturbed by a large set of radiopaque pellets that overlap anatomical structures of interest.

For overcoming these limitations, attempts have been made of using small calibration objects or eliminating them at all. Kadoury *et al.* [Kadoury, Cheriet, Dansereau, and Labelle (2007)] adapted a method previously proposed by Cheriet *et al.* [Cheriet, Dansereau, Petit, Aubin, Labelle, and De Guise (1999)] where no calibration object is used. Calibration is achieved through the minimisation of the retro-projection error of a set of landmarks manually identified in two radiographs. The authors were able of calculating several angular measures of the spine (e.g. Computerised Cobb angle, kyphosis, and lordosis) with no significant differences from the method described in [Cheriet, Laporte, Kadoury, Labelle, and Dansereau (2007)]; however, absolute measures, such as the spinal length, scored very poor results (RMS error of 14.19 mm). This shows that the method was not able of determining scale. For tackling this issue, Kadoury *et al.* enhanced their previous method by using a small calibration object for (i) obtaining an initial guess of the geometrical parameters and (ii) correcting scale [Kadoury, Cheriet, Laporte, and

Labelle (2007)]. With this approach, spinal length was still significantly different; however, errors were much lower (RMS error of 2.05 mm) than when not using calibration objects. To the best of our knowledge, no method has yet achieved this level of errors without using calibration objects.

This paper proposes a new method for addressing the problem of calibration of biplanar radiography of the spine while minimising the need of calibration objects. For accomplishing this, a novel approach is proposed that consists in extending a conventional x-ray system with a measuring device (e.g. a laser rangefinder). This device enables a better estimation of the geometry of the radiological setup without interfering with the content of radiographs. The proposed system is targeted for compatibility with conventional radiological setups, while it may also be used with portable x-ray systems. Therefore, it is here assumed that a rotatory platform is not necessary for positioning patients.

The proposed method is composed by a main core, which includes the geometric parameters estimation from an initial guess given by a measuring device, and two optional components: parameters optimisation, and scale correction. These two components were included with the goal of providing more accurate reconstructions but at the cost of user intervention (in the first case) and a small calibration object (in the second case). This paper reports results of experiments with different configurations of the method (both computer simulations and *in vitro*) for determining the tradeoff of using these optional components, and compares results of the more advantageous configurations with previous calibration methods.

## 2 Materials and methods

The proposed calibration method extends a standard imaging system of planar radiography by enabling 3D reconstructions of the spine. The main components and processes are illustrated by Fig. 1. While some of these are optional (processes inside gray boxes), the complete system will be described here, and in section 3 the tradeoffs of skipping the optional processes will be analysed and discussed.

The input data are two radiographs (Frontal and Lateral) of the patient's spine in digital format, the distance between the x-ray source and the x-ray table measured with a measuring device (e.g. rangefinder) during the radiographs acquisition, and a set of geometric parameters of the radiographic system that are constant and therefore only need to be determined once for a given system. These parameters together with the distance from the measuring device are used to obtain an initial guess of the geometric parameters of the radiological setup.

The identification of the calibration object and of the anatomical landmarks is done manually using a computer software. These landmarks are six corresponding points

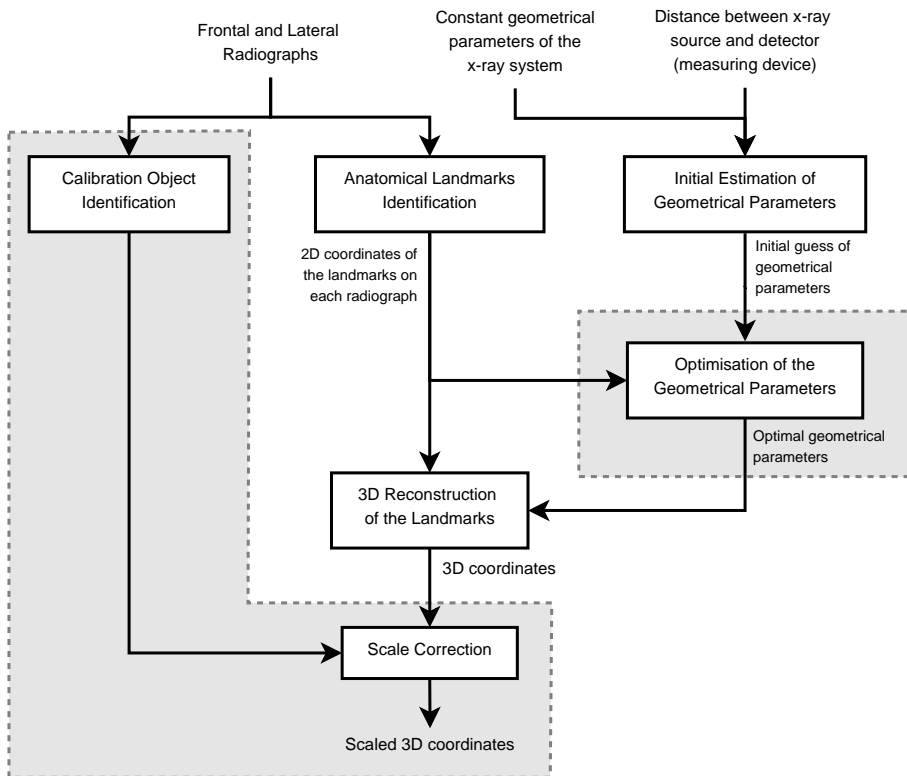


Figure 1: Data flow diagram of the reconstruction system (the calibration processes that are inside gray boxes are optional).

per vertebrae that are visible on both radiographs (i.e. centre of superior and inferior endplates, and the superior and inferior extremities of the pedicles) and that are widely used on methods for reconstructing the spine from biplanar radiography (e.g. [Aubin, Descrimes, Dansereau, Skalli, Lavaste, and Labelle (1995); Mitton, Landry, Veron, Skalli, Lavaste, and De Guise (2000); Kadoury, Cheriet, Dansereau, and Labelle (2007); Kadoury, Cheriet, Laporte, and Labelle (2007); Delorme, Petit, de Guise, Labelle, Aubin, and Dansereau (2003); Mitulescu, Skalli, Mitton, and De Guise (2002); Bras, Laporte, Mitton, de Guise, and Skalli (2003)]).

These data feed a self-calibration process that optimises the geometric parameters of the radiological setup previously estimated. Using these parameters, the 3D coordinates of the anatomical landmarks are obtained by stereo-triangulation with the linear least-squares algorithm [Hartley and Sturm (1997)]. Finally, a calibration object may be used for correcting the scale of the 3D reconstruction.

## **2.1 Radiographs acquisition procedure**

The proposed method requires two orthogonal radiographs of the spine, one AP (Antero-posterior) or PA (Postero-anterior), and one Lateral (Left-right or Right-left). These planes are commonly used by physicians for the follow-up of spinal deformities, such as scoliosis [Cassar-Pullicino and Eisenstein (2002); Greenspan (2004)], and, therefore, the proposed method does not subject patients to additional radiation.

The radiographs acquisition procedure starts by positioning the patient. For guaranteeing a proper positioning without using a rotatory platform, we suggest the same option as [Kadoury, Cheriet, Laporte, and Labelle (2007)], which consists on using markers on the floor for patients to place their feet (Fig. 2). These markers help stabilising patients by making legs to be apart by a considerable distance. Additionally, they allow to have a rough estimation of the distance between the patient's spine and the x-ray table ( $d_p$ ). After positioning the patient, the technician should adjust the distance between the x-ray source and the patient for best fitting the region of interest in the radiographs. After selecting this distance, the first radiograph takes place, followed by a 90 degrees rotation of the patient with the help of the foot-markers for acquiring the second radiograph. Finally, the patient leaves the system, which allows the technician to measure the distance between x-ray source and the x-ray table. We propose measuring this distance with a laser rangefinder for higher accuracy and because it is faster and more practical than using other measuring devices such as metric tapes. This distance will be used to estimate some of the geometric parameters of the system (see section 2.3).

During the acquisition of the radiographs the patient may wear a calibration object that undergoes the same geometrical transformation that the patient experiences

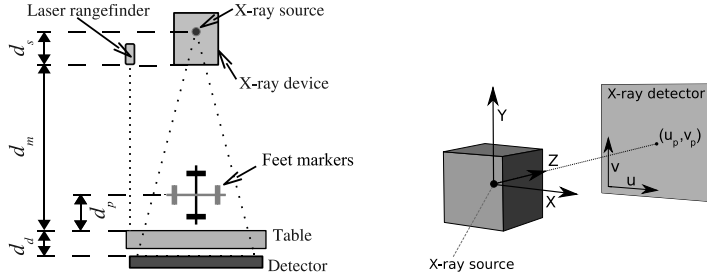


Figure 2: Left: Illustration of a conventional radiographic imaging system (top view) with a laser rangefinder attached. The markers where patients should place their feet are also represented (gray markers for the frontal radiograph; black markers for the lateral radiograph). Right: the coordinate system of reference.

when rotating from the first to the second radiograph. This object should be placed on the lumbar area of the backs of the patient for minimal overlapping with bone structures (i.e. rib cage) and facilitating its identification.

## 2.2 Analytical description of the calibration goal

In biplanar x-ray systems, the projection of a 3D point on each of the two radiographs may be formulated as:

$$\begin{bmatrix} w_i \cdot u_i \\ w_i \cdot v_i \\ w_i \end{bmatrix} = M_i \cdot \begin{bmatrix} X \\ Y \\ Z \\ 1 \end{bmatrix} \quad \text{for } i = 1, 2 \quad (1)$$

where for each acquisition  $i$ ,  $M$  is the calibration matrix that describes the projection of the 3D point  $(X, Y, Z)$  into image coordinates  $(u, v)$  subjected to a scaling factor  $w$ . For flat x-ray detectors,  $M$  may be modelled as:

$$M_i = \begin{bmatrix} f_i/s & 0 & u_{p_i} & 0 \\ 0 & f_i/s & v_{p_i} & 0 \\ 0 & 0 & 1 & 0 \end{bmatrix} \cdot \begin{bmatrix} \mathcal{R}_i & t_i \\ 0_3^T & 1 \end{bmatrix} \quad \text{for } i = 1, 2 \quad (2)$$

where  $f$  is the focal distance (the distance between the x-ray source and the detector),  $s$  is the known sampling pitch of the detector,  $(u_p, v_p)$  is the principal point (2D projection of the x-ray source in the image), and  $\mathcal{R}$  and  $t$  define the geometrical transformation (represented by a  $4 \times 4$  matrix) that aligns the patient's coordinate system with the coordinate system of the x-ray source. More precisely,  $0_3^T$  represents  $(0, 0, 0)^T$ ,  $t$  is a translation vector that may be decomposed in  $(t_x, t_y, t_z)^T$

and  $\mathcal{R}$  is a  $3 \times 3$  rotation matrix. Using Rodrigues' formula, this matrix may be represented by a 3D vector  $\vec{\omega} = (\omega_x, \omega_y, \omega_z)^T$ , which defines a rotation around an axis of direction  $\vec{\omega}$  with magnitude  $\|\vec{\omega}\|$  (numerical implementation details concerning conversions between rotation matrices and 3D vectors using Rodrigues' formula can be found in [Lepetit and Fua (2005)]).

The goal of the calibration procedure is to find the values of the calibration parameters  $\zeta_i$ :

$$\zeta_i = (f_i, u_{p_i}, v_{p_i}, t_{x_i}, t_{y_i}, t_{z_i}, \omega_{x_i}, \omega_{y_i}, \omega_{z_i}) \quad \text{for } i = 1, 2 \quad (3)$$

### 2.3 Initial estimation of the geometric parameters

In a radiographic system where the acquisition setup is not fixed, i.e. focal distance may vary from exam to exam, all the parameters may be reasonably estimated with the exception of the focal distance ( $f$ ), and the distance between the patient's spine and the x-ray source ( $t_z$ ). For the other parameters, one may assume that the principal point ( $u_p, v_p$ ) is located at the centre of radiographs (in pixels), that the patient's spine is centred on both radiographs ( $t_x = 0$  mm,  $t_y = 0$  mm) and that in the frontal radiograph the patient is parallel to the x-ray detector (e.g.  $\omega_{x_1} = 0^\circ$ ,  $\omega_{y_1} = 0^\circ$ ,  $\omega_{z_1} = 0^\circ$ ), and in the lateral (s)he experiences a 90 degrees rotation around the  $Y$  axis (e.g.  $\omega_{x_2} = 0^\circ$ ,  $\omega_{y_2} = 90^\circ$ ,  $\omega_{z_2} = 0^\circ$ ).

For determining the missing parameters ( $f$  and  $t_z$ ) we propose using an off-the-shelf rangefinder. However, in order for using such device, a pre-calibration procedure must first take place. This procedure, described in [Moura, Barbosa, Tavares, and Reis (2008)], only needs to be executed once for a given x-ray system and accurately determines two other geometric parameters (illustrated by Fig. 2) that are constant but essential for determining  $f$  and  $t_z$ :

- $d_s$  – the distance from the x-ray source to the plane of the x-ray device where the x-rays come out;
- $d_d$  – the distance from the table to the x-ray detector.

Having  $d_s$  and  $d_d$  calculated for a given system, converting the distance measured by the rangefinder ( $d_m$ ) into  $f$  and  $t_z$  is very straightforward:

$$f_i = d_s + d_m + d_d, \quad t_{z_i} = d_s + d_m - d_p, \quad \text{for } i = 1, 2 \quad (4)$$

While the focal distance is accurately calculated,  $t_z$  is only an approximated value that depends of the patient's positioning (this happens because  $d_p$  is given by the floor markers described on subsection 2.1, which represent the expected distance of the patient's spine to the x-ray table).

At this stage, rough values are available for all geometric parameters  $\zeta_i$  (with the exception of  $f$ , which is accurately known) and, therefore, the 3D coordinates of the landmarks identified on both radiographs may already be obtained by stereo-triangulation. Nevertheless, 3D reconstructions obtained directly from this estimation of  $\zeta_i$  may suffer from errors of the patient's positioning. This problem is addressed by the next section.

#### 2.4 Optimisation of the geometric parameters

In an attempt of improving the initial estimation of the geometric parameters the proposed method may include an optimisation process that iteratively updates the geometric parameters, towards minimizing the retro-projection error of the identified anatomical landmarks [Cheriet, Dansereau, Petit, Aubin, Labelle, and De Guise (1999); Kadoury, Cheriet, Dansereau, and Labelle (2007); Kadoury, Cheriet, Laporte, and Labelle (2007)]. Since the focal distance is already known, and small errors on the principal point can be compensated by a translation, we choose not to include these parameters on the optimisation process in order to reduce the search space of solutions. Therefore, the new set of parameters to optimise may be defined as:

$$\xi_i = (t_{x_i}, t_{y_i}, t_{z_i}, \omega_{x_i}, \omega_{y_i}, \omega_{z_i}) \quad \text{for } i = 1, 2 \quad (5)$$

The above problem may be formulated as a least-squares minimisation:

$$\min_{\xi_1^*, \xi_2^*} \left( \sum_{i=1}^2 \sum_{j=1}^n \|p_{ij} - prj(\xi_i, tri(\xi_1, \xi_2, p_{1j}, p_{2j}))\|^2 \right) \quad (6)$$

where  $n$  is the number of point matches (anatomical landmarks),  $p_{ij}$  is the  $j^{\text{th}}$  landmark identified on image  $i$ ,  $prj$  is the 2D projection of a 3D point as defined in equations 1 and 2,  $tri$  is a triangulation operation that calculates the 3D coordinates for a given point match, and  $\xi_1^*, \xi_2^*$  are the optimised parameters for the frontal and lateral radiographs respectively.

This minimisation problem was solved using Matlab's implementation of the Trust-region-reflective method [Coleman and Li (1996)] for nonlinear least-squares problems. This method allows to define bounds for the parameters being optimised that limit the search space of solutions even further. In our experiments, it achieved a superior performance than the commonly used Levenberg-Marquardt algorithm [Marquardt (1963)], both in terms of processing time and quality of the final solution.

The optimisation procedure just described should be able of improving reconstruction results and should compensate patient's positioning errors. However, it does

Table 1: Side of the patient where the calibration object should be placed according to the patient's orientation on the frontal and lateral radiographs (e.g. if the patient is subjected to Antero-posterior and Left-right radiographs, the object should be placed on the left side of his backs).

	Left-right x-ray	Right-left x-ray
Antero-posterior x-ray	Left side	Right side
Postero-anterior x-ray	Right side	Left side

not guarantee that scale is correctly recovered. This issue will be addressed on the next section.

## 2.5 Scale correction

Calibration methods that do not use calibration objects usually are not able of handling scale [Kadoury, Cheriet, Dansereau, and Labelle (2007); Cheriet, Dansereau, Petit, Aubin, Labelle, and De Guise (1999)]. For correcting the scale of the 3D reconstruction, we propose using a very simple calibration object that only needs to have two radiopaque pellets at a known distance. This provides minimal impact on the content of radiographs. The scaling factor may be calculated as the ratio between the real distance between the two pellets and the distance between the reconstructed 3D coordinates of the pellets identified on both radiographs.

Experimentally it was determined that for best results the object should be placed upright (like illustrated on Fig. 3). Additionally, the object should be positioned according to the orientation of the patient in both radiographs (like described on Tab. 1).

## 2.6 Evaluation using Simulation with in vivo 3D data

The evaluation of the proposed method was first done simulating radiographic exams with an *in vivo* CT scan of a woman with 77 years old<sup>1</sup>. The CT scan captures the complete thoracic and lumbar spine with voxel size of  $0.4 \times 0.4 \times 0.5 \text{ mm}^3$ . The anatomical landmarks were manually identified by a human expert on the CT scan for vertebrae T1 to L5, and constitute the ground truth for this study. For simulating radiographs acquisitions on realistic conditions, Gaussian noise was added to the geometric parameters and to the landmarks, which were then projected to the Antero-posterior and Left-right planes for simulating the 2D landmarks that the method receives as input. No noise was added to the landmarks of the calibration

<sup>1</sup> This exam was retrieved from a database of clinical exams and, therefore, it was not especially acquired for this experiment nor for clinical trials.

Table 2: Standard deviation of the Gaussian noise that was added to the geometric parameters on simulations.

Geometric parameters	Noise 1 <sup>st</sup> experience (Controlled Setup)	Noise 2 <sup>nd</sup> experience (Pessimistic Scenario)
Rotation ( $\omega_x, \omega_y, \omega_z$ )	0.5°	2.0°
Translation ( $t_x, t_y, t_z$ )	4.0 mm	8.0 mm
Principal point ( $u_p, v_p$ )	2.0 mm	4.0 mm
Focal distance ( $f$ )	1.5 mm	1.5 mm

object since radiopaque pellets can be precisely identified on radiographs.

Two experiments were done with different levels of noise (Tab. 2). In the first (Controlled Setup), the same amount of noise used on [Kadoury, Cheriet, Laporte, and Labelle (2007)] was considered for all geometric parameters except focal length, which in our case can be accurately calculated using the rangefinder. Therefore, the noise on the focal length was based on the accuracy specifications of an off-the-shelf laser rangefinder (S.D. of the error of 1.5 mm). In a second experiment (Pessimistic Scenario) the geometric errors were increased (with the exception of focal length) using the maximum expected variation on this kind of clinical setups [Kadoury, Cheriet, Laporte, and Labelle (2007)]. On both experiences, the amount of noise added to the anatomical landmarks had standard deviation of 1 mm, which is the expected for landmarks identified by a human expert [Kadoury, Cheriet, Laporte, and Labelle (2007)]. The bounds used on the optimisation algorithm were set to 4 times the S.D. of the noise added to the corresponding geometric parameters.

For each experiment 100 trials were simulated and, for each trial, random Gaussian noise was added to both parameters and landmarks. The calibration object length was 120 mm and, for each trial, it was randomly placed in the left side of the lumbar area of the patient. For simulating real conditions, Gaussian noise was also added to the object orientation (standard deviation of 2.4°). Fig. 3 illustrates a simulation of a single exam and the correspondent 3D reconstruction.

Two measures were used for assessing the reconstruction quality: the 3D reconstruction error of each landmark (after rigidly aligning the reconstruction with the ground truth), and the 3D spinal length [Papin, Labelle, Delorme, Aubin, De Guise, and Dansereau (1999)]. This last clinical index was included on this study because of difficulties of previous methods [Kadoury, Cheriet, Dansereau, and Labelle (2007)] on determining it. It is calculated by summing the euclidian distances between every pair of consecutive vertebral bodies' centres, which, on their turn, are calculated as the midpoint between the superior and inferior centres of the vertebra's endplates.

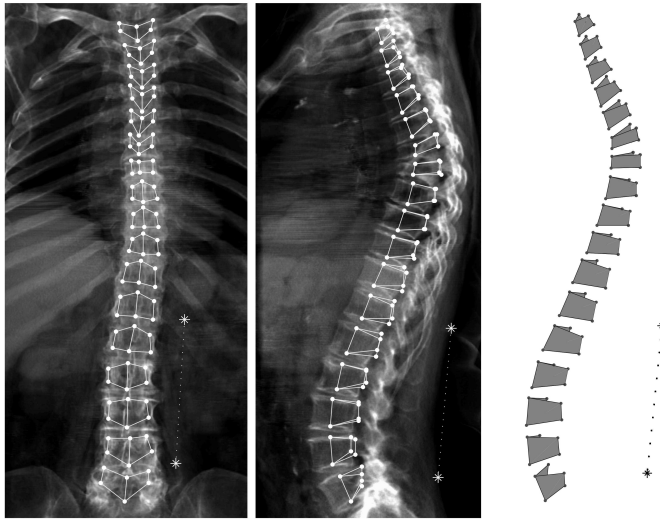


Figure 3: Left – example of digitally reconstructed radiographs (Antero-posterior and Left-right) for the CT scan used on the simulation with the anatomical landmarks (filled dots) and a representation of the optional calibration object (asterisks). Right – 3D reconstruction.

For determining the gain and need of using the different components of the proposed method (i.e. the rangefinder, the optimisation process, and the calibration object), different setups were experimented according to the following list:

1. **Initial Error:** the reconstruction was performed by triangulating the noisy anatomical landmarks, with no optimisation of the geometric parameters and no scale correction. For simulating that no rangefinder was being used, the noise on focal distance was set to S.D. 20 mm on the first experiment (controlled radiological setup) and to 40 mm on the second experiment (pessimistic scenario) [Kadoury, Cheriet, Laporte, and Labelle (2007)];
2. **Rangefinder:** same as Setup 1, but the S.D. of the focal distance was decreased to 1.5 mm to simulate the use of a simple rangefinder;
3. **Rangefinder and Calibration Object:** same as Setup 2, but after triangulating the landmarks they were scaled using the calibration object;
4. **Rangefinder and Optimisation:** same as Setup 2, but before triangulating the landmarks the geometric parameters were optimised;

5. **Complete Process:** equivalent to Setup 4, followed by scale correction with the calibration object.

In addition, an experiment was made to evaluate the effect of the precision of the measuring device on the quality of the reconstruction. This experiment was done using the noise settings of the pessimistic scenario, simulating an increasing range of noise on the measuring device.

### 2.7 In vitro validation

Finally, the method was validated using 17 dried vertebrae (T1-L5) of a human with unknown age, which were disposed in order to resemble a typical spine (Fig. 4). A calibration bar of length 122.3 mm was used for scaling the final 3D reconstruction. The spine was first scanned using CT (voxel size of  $0.4 \times 0.4 \times 0.3 \text{ mm}^3$ ) and then radiographed in the AP and Right-left planes (pixel size  $0.1750 \times 0.1750 \text{ mm}^2$ ) using a film holder for large radiographs. The holder enables to have 3 films with dimensions of  $14'' \times 14''$ , which are then scanned separately and finally merged. For this experiment only 2 films were needed to capture the complete spine. When acquiring the radiographs, an off-the-shelf laser rangefinder (a Bosh DLE 50, which has a typical error of  $\pm 1.5 \text{ mm}$ , maximum error of  $\pm 3.0 \text{ mm}$ , and range of operation of 0.05–50m) was used to measure distance  $d_m$  (Fig. 2). Especial concern was taken on using a low cost and standard rangefinder. Then, all landmarks were identified in both CT and radiographs by an expert. The proposed method was used to reconstruct the 3D coordinates of the anatomical landmarks, which were then rigidly aligned and compared with the landmarks of the CT scan. The 3D spinal length was also evaluated. Moreover, the same variants of the method that were used in the simulations were included in this experiment for confronting both studies.

## 3 Results and Discussion

Results of the simulated experiments (Fig. 5) show RMS 3D reconstruction errors between 1.6 mm and 1.7 mm for the Controlled Setup and between 1.9 mm and 2.0 mm for the Pessimistic Scenario. These results revealed that the use of a simple rangefinder by itself (with no calibration object nor parameters optimisation) enables achieving practically the same 3D reconstruction errors than the complete process. This was confirmed by the *in vitro* experiments where the RMS 3D reconstruction error when using only the rangefinder was of 1.9 mm and for the other variants of the method was 1.8 mm (Fig. 6). However, simulation errors for the spinal length in the Pessimistic Scenario were considerably higher than when using the complete process (2.87 mm vs 2.09 mm), but still acceptable. This is a ma-

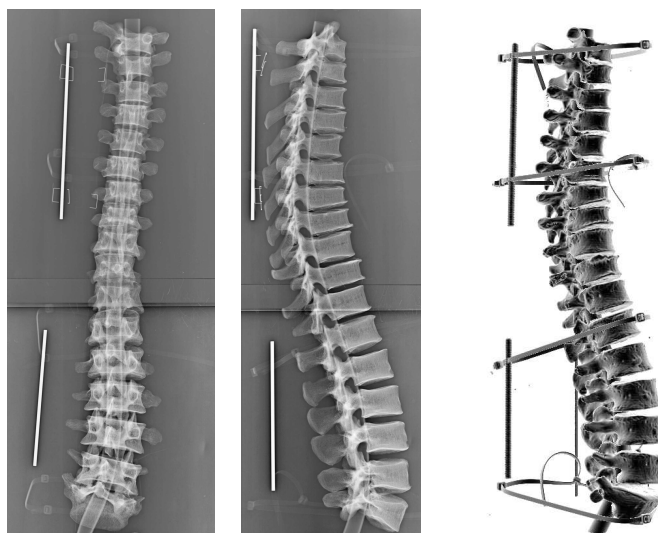


Figure 4: Radiographs of the dried vertebrae with the calibration bar (AP and Lateral), and reconstruction from the CT scan. Only the bottom bar was used on the experiments reported here.

for improvement over previous work, since results obtained by calibration methods that do not use calibration objects scored an error of 14.19 mm when measuring the spinal length (for *in vivo* experiments) [Kadoury, Chretien, Dansereau, and Labelle (2007)]. Once again, the *in vitro* experiments were consistent with the conclusions of the simulation study.

From these experiments it is also possible to conclude that, when using a rangefinder, scaling the reconstruction using a small calibration object and optimising the geometrical parameters only seem to be considerably advantageous when used together. This is especially observable on the simulation of the Pessimistic Scenario, where only the complete version of the process achieved a considerably lower error on the spinal length when compared to the version that only used the rangefinder. Therefore, on further comparisons with other methods, only two variants will be considered: a) using only the rangefinder, and b) the complete process.

Experiments with different ranges of noise on the measuring device (Fig. 7) show that there is a clear relation between the precision of the device and the quality of the reconstruction. As expected, this relation is particularly noticeable when not using a calibration object since no scale correction is done. In these cases, the use of a laser range-finder such as the one that was used in the *in vitro* experiments (with S.D. of 1.5 mm) is advised. However, when using a calibration object to cor-

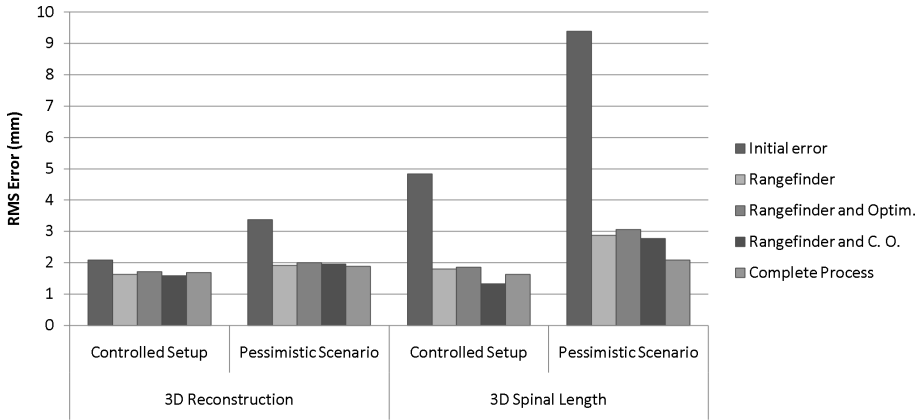


Figure 5: Simulation results for the comparison of 3D Reconstruction and Spinal Length errors of different configurations of the proposed method, for two different scenarios (detailed in Tab. 2).

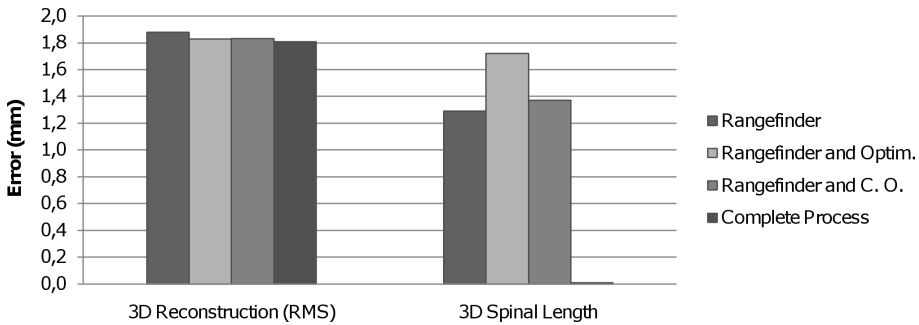


Figure 6: *In vitro* results for the comparison of 3D Reconstruction and Spinal Length errors of different configurations of the proposed method. The error of the spinal length when using the complete process is hardly visible because it only scored 0.01 mm.

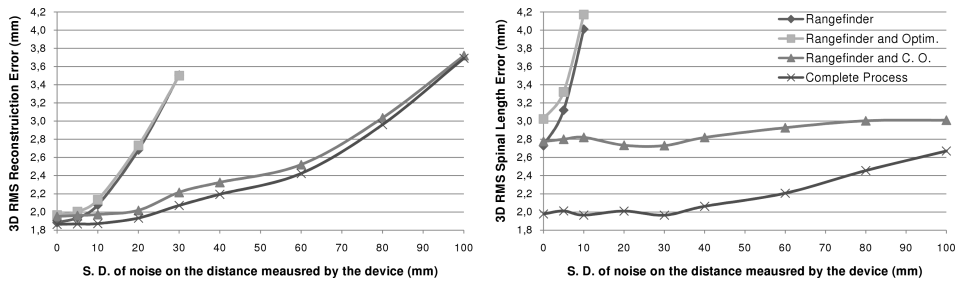


Figure 7: Simulation results for the evaluation of the effect of the precision of the measuring device on the 3D reconstruction error (left) and on the 3D spinal length (right).

rect scale, such precision is not necessary since the method shows no considerable increase of reconstruction errors up to a S.D. of the noise of 10.0 mm. Nevertheless, this experiment clearly shows that even when using a calibration object and optimising the calibration parameters it is important to have a good initial value of the focal distance. Moreover, it validates the hypothesis that the measuring device is the key component for simplifying the method by discarding the scale correction and/or the optimisation of the parameters.

Reconstruction errors for the simulations on the Controlled Setup (1.6 mm when only using the rangefinder and 1.7 mm for the complete process) were slightly lower than the 1.8 mm reconstruction error achieved on the simulations presented in [Kadoury, Cheriet, Laporte, and Labelle (2007)] with similar noise levels (with the exception of focal length that has less noise in our case due to the use of a rangefinder). Despite this difference may be explained by factors that are difficult to replicate (e.g. source of 3D data), it shows that the methods have a comparable performance. However, while the method proposed in [Kadoury, Cheriet, Laporte, and Labelle (2007)] needs a set of landmarks for optimising the geometrical parameters and uses a calibration object of  $100 \text{ mm} \times 70 \text{ mm}$  that slightly overlaps bone structures, it has been shown here that the rangefinder per se enables achieving similar performances in terms of 3D reconstructions for this level of noise.

Simulation results also show that the error on the spinal length also compares well with the *in vivo* results of [Kadoury, Cheriet, Laporte, and Labelle (2007)] where the authors obtained a RMS error of 2.05 mm. This was approximately the same value that the complete version of the proposed method achieved when simulating a Pessimistic Scenario (2.09 mm), with the advantage of using a calibration object with lower impact on the content of radiographs, and the disadvantage of needing a rangefinder. When using only the rangefinder the error of the spinal length was

higher (2.87 mm). However, it is difficult to make a fair comparison with *in vivo* studies since there is no ground truth available. Additionally, the calculation of clinical indices by the use of manually identified points has considerable intra and inter-observer variability (RMS of 1.8 mm and 2.6 mm respectively for the spinal length [Delorme, Petit, de Guise, Labelle, Aubin, and Dansereau (2003)]). Moreover, in the *in vivo* validation performed in [Kadoury, Cheriet, Laporte, and Labelle (2007)], patients were positioned by the use of a rotatory platform, which decreases positioning errors.

In terms of robustness, simulations show that both variants handled an increase of noise by a factor of 2 in most of the parameters and by a factor of 4 on rotation (from the Controlled Setup to the Pessimistic Scenario) by only increasing the RMS 3D reconstruction error by factors of 1.12 on the complete version of the method, and 1.18 when only using the rangefinder. In terms of the spinal length, the method shown higher sensibility, especially when only using a rangefinder (increasing factor of 1.60 vs 1.29). This shows, as expected, that when using only a rangefinder, the method is more sensible to errors on the initial estimation of the geometric parameters and, therefore, proper patient positioning is more crucial than in the complete version of the proposed method.

*In vitro* results (Tab. 3) also compare well with results from large calibration apparatus, like is the case of [Aubin, Dansereau, Parent, Labelle, and de Guise (1997)]. As expected, the 3D reconstruction errors of the proposed method are higher (mean error of 1.7 mm vs 1.3 mm), since the method presented in [Aubin, Dansereau, Parent, Labelle, and de Guise (1997)] uses a calibration cage that completely surrounds the patient, and a rotatory platform that guarantees low rotation errors when positioning patients. On the other hand, the proposed method offers several advantages that may justify the loss of exactness, such as, much lower costs, superior user-friendliness, compatibility with standard radiological systems, and much less (or no) artifacts on radiographs overlapping anatomical structures. Additionally, while the complete version of the proposed method is able of handling patient motion between radiographs, the same does not happen with the cage method (as it was shown in [Cheriet, Laporte, Kadoury, Labelle, and Dansereau (2007)]).

The results from the experiments reported here do not allow making direct comparisons with other calibration methods that use large calibration apparatus because of different evaluation measures. However, both [Dumas, Mitton, Laporte, Dubousset, Steib, Lavaste, and Skalli (2003)] and [Cheriet, Laporte, Kadoury, Labelle, and Dansereau (2007)] had comparable performances to [Aubin, Dansereau, Parent, Labelle, and de Guise (1997)], which let us generalise the conclusions of the previous comparison. The major exception is the method proposed in [Cheriet, Laporte, Kadoury, Labelle, and Dansereau (2007)], which is also able of handling patient

Table 3: 3D reconstruction errors (mean±S.D. in *mm*) of the *in vitro* validation, and comparison with *in vitro* results using a large calibration apparatus that surrounds the patient [Aubin, Dansereau, Parent, Labelle, and de Guise (1997)]. The last line shows the reconstruction errors for the complete set of anatomical landmarks (S.D. not published in [Aubin, Dansereau, Parent, Labelle, and de Guise (1997)] for this set of landmarks).

	Rangefinder	Rangefinder Optim., C.O.	Large apparatus Aubin <i>et al.</i> (1997)
Plates	1.7±0.6	1.7±0.6	1.5±0.7
Pedicles	1.8±0.8	1.6±0.8	1.2±0.7
All landmarks	1.7±0.7	1.7±0.7	1.3

motion.

The errors presented here may increase on *in vivo* clinical conditions if patient positioning is not properly done. Additionally, for the complete version of the method, landmarks identification errors may be higher in areas where vertebrae are not so visible due to overlapping bone structures (e.g. upper thoracic vertebrae on lateral radiographs). However, an *in vivo* validation is not possible because conventional 3D imaging techniques (e.g. CT, MRI) are unsuitable since they alter the spine configuration, and gold-standard calibration apparatus are only available in very few health institutions.

Summarising, the method proposed here may be used in two particularly advantageous configurations. In the first, the rangefinder is used to help estimating the geometrical parameters, which are then directly used for performing the 3D reconstruction. In this version of the method, special care should be given to patient positioning, but there is no need for calibration objects. Additionally, no landmarks are necessary. The advantages are twofold: a source of error is eliminated, and user intervention is drastically reduced. One may argue that landmarks are still necessary for the reconstruction process; however, other reconstruction methods that are urging and that require much less supervision [Dumas, Blanchard, Carlier, de Loubresse, Le Huec, Marty, Moinard, and Vital (2008); Humbert, Guise, Aubert, Godbout, and Skalli (2009); Kadoury, Cheriet, and Labelle (2009); Moura, Boisvert, Barbosa, and Tavares (2009); Benameur, Mignotte, Labelle, and Guise (2005); Benameur, Mignotte, Parent, Labelle, Skalli, and de Guise (2003)] may be used for accomplishing this. As for the second version of the proposed method, all components described in section 2 are used, that is, the geometrical parameters are optimised and scale is corrected using a small calibration object. This version turned out to be more robust and accurate. However, it needs a considerably

large set of points to be identified and patients must wear a calibration object. This set of points is no larger than sets required by other methods [Kadoury, Chretien, Dansereau, and Labelle (2007); Kadoury, Chretien, Laporte, and Labelle (2007)]. Moreover, for the set of measures under study, using a simple rangefinder enabled to achieve performances comparable to the method proposed in [Kadoury, Chretien, Laporte, and Labelle (2007)], while requiring a much simpler calibration object that has smaller impact on the content of radiographs.

#### **4 Conclusion**

This paper presented a calibration method that estimates the geometrical parameters of a conventional radiological system and thus enables performing 3D reconstructions of the spine. This method may be implemented in any clinical institution without requiring especial positioning equipment, while it remains sufficiently accurate for carrying out evaluation and follow-up exams of spinal deformities, and planning subsequent clinical interventions (e.g. surgery, braces assessment and design).

In this study it was shown that, for the first time, accurate 3D reconstructions of the spine with correct scale may be achieved from biplanar radiographs without calibration objects. This was possible due to the introduction of an off-the-shelf laser rangefinder that is used for estimating some of the geometrical parameters of the radiological setup, with just one measurement per examination. It was also shown that, for the first time, accurate calibrations without calibration objects are possible without the need of an expert for identifying anatomical landmarks on radiographs. This makes this approach especially attractive since many clinical institutions may not afford having an expert allocated to this task, which is very time-consuming, subjective and error-prone.

For superior accuracy and robustness, the method benefits from two optional steps: an optimisation of the geometrical parameters followed by a scale adjustment using a very simple calibration object. The optimisation is especially useful for compensating changes of posture of the patient between radiographs, whereas the calibration object guarantees that scale is correct. However, the optimisation procedure requires a set of anatomical landmarks to be identified by an expert, which has the previously mentioned disadvantages. Results with these enhancements are comparable with previous techniques that require similar user intervention, whereas in the proposed method the use of rangefinder enabled to simplify the geometry of the calibration object. This is particularly important since only two radiopaque pellets of a single calibration object need to be visible on both radiographs, which produces minimal changes to radiographs without overlapping anatomical structures of interest.

The method presented here was first validated using computer simulations based on *in vivo* CT data. Additionally, an *in vitro* study was performed where reconstructions using the proposed method on a conventional radiological system were compared with reconstructions from CT. The obtained results show that the method is suitable for clinical use.

## 5 Acknowledgements

The first author thanks Fundação para a Ciência e a Tecnologia for his PhD scholarship (SFRH/BD/31449/2006). This work was partially carried out under the scope of the projects entitled "Methodologies to Analyze Organs from Complex Medical Images - Applications to the Female Pelvic Cavity", "Aberrant Crypt Foci and Human Colorectal Polyps: mathematical modelling and endoscopic image processing" and "Cardiovascular Imaging Modeling and Simulation - SIMCARD", with references PTDC/EEA-CRO/103320/2008, UTAustin/MAT/0009/2008 and UTAustin/CA/0047/2008, respectively, financially supported by the Fundação para a Ciência e Tecnologia.

## References

- Abdel-Aziz, Y.; Karara, H.** (1971): Direct linear transformation from comparator coordinates into object space coordinates in close-range photogrammetry. In *Proc. Symposium on Close-Range Photogrammetry*, pp. 1–18.
- Aubin, C.; Dansereau, J.; Parent, F.; Labelle, H.; de Guise, J. A.** (1997): Morphometric evaluations of personalised 3D reconstructions and geometric models of the human spine. *Med. Biol. Eng. Comput.*, vol. 35, no. 6, pp. 611–618.
- Aubin, C.-E.; Descrimes, J.-L.; Dansereau, J.; Skalli, W.; Lavaste, F.; Labelle, H.** (1995): Geometrical modelling of the spine and thorax for biomechanical analysis of scoliotic deformities using finite element method. *Ann. Chir.*, vol. 49, no. 8, pp. 749–761.
- Benameur, S.; Mignotte, M.; Labelle, H.; Guise, J. A. D.** (2005): A hierarchical statistical modeling approach for the unsupervised 3-D biplanar reconstruction of the scoliotic spine. *IEEE Trans. Biomed. Eng.*, vol. 52, no. 12, pp. 2041–2057.
- Benameur, S.; Mignotte, M.; Parent, S.; Labelle, H.; Skalli, W.; de Guise, J.** (2003): 3D/2D registration and segmentation of scoliotic vertebrae using statistical models. *Comput. Med. Imag. Grap.*, vol. 27, no. 5, pp. 321–337.
- Bras, A. L.; Laporte, S.; Mitton, D.; de Guise, J. A.; Skalli, W.** (2003): Three-dimensional (3D) detailed reconstruction of human vertebrae from low-dose digital stereoradiography. *Eur. J. Orthop. Surg. Traumatol.*, vol. 13, no. 2, pp. 57–62.

**Cassar-Pullicino, V.; Eisenstein, S.** (2002): Imaging in scoliosis: What, why and how? *Clin. Radiol.*, vol. 57, no. 7, pp. 543–562.

**Cheriet, F.; Dansereau, J.; Petit, Y.; Aubin, C.; Labelle, H.; De Guise, J. A.** (1999): Towards the self-calibration of a multiview radiographic imaging system for the 3D reconstruction of the human spine and rib cage. *Int. J. Pattern Recognit Artif Intell.*, vol. 13, no. 5, pp. 761–779.

**Cheriet, F.; Laporte, C.; Kadoury, S.; Labelle, H.; Dansereau, J.** (2007): A novel system for the 3-D reconstruction of the human spine and rib cage from biplanar x-ray images. *IEEE Trans. Biomed. Eng.*, vol. 54, no. 7, pp. 1356–1358.

**Coleman, T. F.; Li, Y.** (1996): An interior trust region approach for nonlinear minimization subject to bounds. *SIAM J. Optim.*, vol. 6, no. 2, pp. 418–445.

**Dansereau, J.; Stokes, I.** (1988): Measurements of the three-dimensional shape of the rib cage. *J. Biomech.*, vol. 21, no. 11, pp. 893–901.

**Delorme, S.; Petit, Y.; de Guise, J.; Labelle, H.; Aubin, C.-E.; Dansereau, J.** (2003): Assessment of the 3-D reconstruction and high-resolution geometrical modeling of the human skeletal trunk from 2-d radiographic images. *IEEE Trans. Biomed. Eng.*, vol. 50, no. 8, pp. 989–998.

**Dumas, R.; Blanchard, B.; Carlier, R.; de Loubresse, C.; Le Huec, J.; Marty, C.; Moinard, M.; Vital, J.** (2008): A semi-automated method using interpolation and optimisation for the 3D reconstruction of the spine from bi-planar radiography: a precision and accuracy study. *Medical and Biological Engineering and Computing*, vol. 46, no. 1, pp. 85–92.

**Dumas, R.; Mitton, D.; Laporte, S.; Dubousset, J.; Steib, J. P.; Lavaste, F.; Skalli, W.** (2003): Explicit calibration method and specific device designed for stereoradiography. *J. Biomech.*, vol. 36, no. 6, pp. 827–834.

**Greenspan, A.** (2004): *Orthopedic Imaging: A Practical Approach*. Lippincott Williams & Wilkins, 4th edition.

**Hartley, R.; Sturm, P.** (1997): Triangulation. *Comput. Vis. Image. Und.*, vol. 68, no. 2, pp. 146–157.

**Humbert, L.; Guise, J. D.; Aubert, B.; Godbout, B.; Skalli, W.** (2009): 3D reconstruction of the spine from biplanar x-rays using parametric models based on transversal and longitudinal inferences. *Med. Eng. Phys.*, vol. 31, no. 6, pp. 681–687.

**Kadoury, S.; Cheriet, F.; Dansereau, J.; Labelle, H.** (2007): Three-dimensional reconstruction of the scoliotic spine and pelvis from uncalibrated biplanar x-ray images. *J. Spinal. Disord. Tech.*, vol. 20, no. 2, pp. 160–167.

- Kadoury, S.; Cheriet, F.; Labelle, H.** (2009): Personalized x-ray 3D reconstruction of the scoliotic spine from hybrid statistical and image-based models. *IEEE Trans. Med. Imag.*, vol. 28, no. 9, pp. 1422–1335.
- Kadoury, S.; Cheriet, F.; Laporte, C.; Labelle, H.** (2007): A versatile 3D reconstruction system of the spine and pelvis for clinical assessment of spinal deformities. *Med. Biol. Eng. Comput.*, pp. 591–602.
- Labelle, H.; Bellefleur, C.; Joncas, J.; Aubin, C.; Cheriet, F.** (2007): Preliminary evaluation of a computer-assisted tool for the design and adjustment of braces in idiopathic scoliosis: A prospective and randomized study. *Spine*, vol. 32, no. 8, pp. 835–843.
- Lepetit, V.; Fua, P.** (2005): Monocular model-based 3D tracking of rigid objects: A survey. *Foundations and Trends in Computer Graphics and Vision*, vol. 1, no. 1, pp. 1–89.
- Marquardt, D. W.** (1963): An algorithm for least-squares estimation of nonlinear parameters. *SIAM J. Appl. Math.*, vol. 11, no. 2, pp. 431–441.
- Mitton, D.; Landry, C.; Veron, S.; Skalli, W.; Lavaste, F.; De Guise, J.** (2000): 3D reconstruction method from biplanar radiography using non-stereocorresponding points and elastic deformable meshes. *Med. Biol. Eng. Comput.*, vol. 38, no. 2, pp. 133–139.
- Mitulescu, A.; Skalli, W.; Mitton, D.; De Guise, J.** (2002): Three-dimensional surface rendering reconstruction of scoliotic vertebrae using a non stereo-corresponding points technique. *Eur. Spine. J.*, vol. 11, no. 4, pp. 344–352.
- Moura, D. C.; Barbosa, J. G.; Tavares, J. M. R. S.; Reis, A. M.** (2008): Calibration of bi-planar radiography with a rangefinder and a small calibration object. In *ISVC08 - 4th International Symposium on Visual Computing*, volume LNCS 5358, pp. 572–581. Springer-Verlag.
- Moura, D. C.; Boisvert, J.; Barbosa, J. G.; Tavares, J. M. R. S.** (2009): Fast 3D reconstruction of the spine using user-defined splines and a statistical articulated model. In *ISVC09 - 5th International Symposium on Visual Computing*, volume LNCS 5875, pp. 586–595. Springer-Verlag.
- Papin, P.; Labelle, H.; Delorme, S.; Aubin, C.; De Guise, J.; Dansereau, J.** (1999): Long-term three-dimensional changes of the spine after posterior spinal instrumentation and fusion in adolescent idiopathic scoliosis. *Eur. Spine. J.*, vol. 8, no. 1, pp. 16–21.
- Perie, D.; Aubin, C.-E.; Petit, Y.; Beausejour, M.; Dansereau, J.; Labelle, H.** (2003): Boston brace correction in idiopathic scoliosis: A biomechanical study. *Spine*, vol. 28, no. 15, pp. 1672–1677.

**Pomero, V.; Mitton, D.; Laporte, S.; de Guise, J. A.; Skalli, W.** (2004): Fast accurate stereoradiographic 3D-reconstruction of the spine using a combined geometric and statistic model. *Clin. Biomech.*, vol. 19, no. 3, pp. 240–247.

**Périé, D.; Aubin, C. E.; Lacroix, M.; Lafon, Y.; Labelle, H.** (2004): Biomechanical modelling of orthotic treatment of the scoliotic spine including a detailed representation of the brace-torso interface. *Medical and Biological Engineering and Computing*, vol. 42, no. 3, pp. 339–344.

**Stokes, I. A.** (1994): Three-dimensional terminology of spinal deformity. a report presented to the scoliosis research society by the scoliosis research society working group on 3-D terminology of spinal deformity. *Spine*, vol. 19, no. 2, pp. 236–248.

**Wood, G.; Marshall, R.** (1986): The accuracy of dlt extrapolation in three-dimensional film analysis. *J. Biomech.*, vol. 19, no. 9, pp. 781–785.

**Yang, C.; Tang, D.; Yuan, C.; Hatsukami, T.; Zheng, J.; Woodard, P.** (2007): In Vivo/Ex Vivo MRI-Based 3D Non-Newtonian FSI Models for Human Atherosclerotic Plaques Compared with Fluid/Wall-Only Models. *CMES: Computer modeling in engineering & sciences*, vol. 19, no. 3, pp. 233.

**Yang, C.; Tang, D.; Yuan, C.; Kerwin, W.; Liu, F.; Canton, G.; Hatsukami, T.; Atluri, S.** (2008): Meshless Generalized Finite Difference Method and Human Carotid Atherosclerotic Plaque Progression Simulation Using Multi-Year MRI Patient-Tracking Data. *CMES: Computer modeling in engineering & sciences*, vol. 28, no. 2, pp. 95.

